[Fe(PMA)]$^{n+}$ (n = 1, 2): Good Models of Fe–Bleomycins and Examples of Mononuclear Non-Heme Iron Complexes with Significant O_2-Activation Capabilities

Richard J. Guajardo, Samuel E. Hudson, Steven J. Brown, and Pradip K. Mascharak*

Contribution from the Department of Chemistry and Biochemistry, University of California, Santa Cruz, California 95064

Received June 29, 1992

Abstract: The Fe(II) and Fe(III) complexes of a designed ligand PMAH that mimics the metal-binding portion of the antitumor drug bleomycin (BLM) have been isolated and characterized by spectroscopic techniques. In both [Fe^{II}(PMA)]Cl·MeOH (**4**) and [Fe^{III}(PMA)](NO$_3$)$_2$·DMSO (**5**), the deprotonated PMA$^-$ framework is ligated to the metal center through five nitrogens located in the primary and secondary amines, pyrimidine and imidazole rings, and the amide moiety. The sixth coordination site on iron in these complexes is occupied by a solvent molecule that is easily replaceable. Similarities in spectral and chemical behaviors of these two model complexes with those of the Fe(II) and Fe(III) complexes of BLM strongly suggest that the drug employs the same set of donor centers to bind iron. For example, **4** binds CO and NO, the former in a reversible manner, and the spectral parameters of the adducts are very similar to those for the corresponding adducts of Fe^{II}–BLM. Most notably, brief exposure of a methanolic solution of **4** to dioxygen generates [(PMA)Fe^{III}–O–OH]$^+$, a low-spin iron(III)–hydroperoxy species which exhibits an EPR spectrum (g = 2.27, 2.18, and 1.93) that is identical with the spectrum of "activated bleomycin". Reaction of **5** with H_2O_2 also affords this species. Like the Fe–BLMs, **4** inflicts strand breaks in DNA in the presence of sodium ascorbate and O_2 while **5** causes strand scission in the presence of H_2O_2. Longer incubation leads to digestion of DNA with the formation of base propenals. Interestingly, Fe–BLMs and the model complexes exhibit the same sequence specificity (5′-G-pyrimidine-3′) in the DNA cleavage reactions. This fact clearly indicates that the primary determinant of the DNA sequence specificity of Fe–BLMs is the metal-binding domain of the metallodrug. The two model complexes also promote rapid oxo transfer to olefinic substrates in stereospecific manner and their oxo transfer capabilities approach those of the Fe–BLMs (and [Fe(TPP)]Cl (TPP = tetraphenylporphyrinato)) under similar experimental conditions. The monooxygenase activity of **4** and **5** is especially noteworthy, since these two are the first examples of *mononuclear* non-heme iron complexes capable of O_2 activation. Reaction of **5** with PhIO in basic media gives rise to [(PMA)Fe^{III}–O–OH]$^+$, a rare example of O–O bond formation at the iron center. Taken together, these results indicate that {hydroperoxo}iron(III) species could be involved in O_2 activation by non-heme iron complexes in general.

Introduction

The bleomycin (BLM, **1**) family of glycopeptide antibiotics is used in combination chemotherapy against several types of cancer.[1] The drug inflicts damage to cellular DNA in the presence of metal ions (like Fe^{2+}) and dioxygen.[2] Oxygenation followed by one-electron reduction of the Fe(II) chelate of BLM results in the formation of "activated bleomycin", an oxygenated low-spin Fe(III) species with a characteristic EPR spectrum.[3] This EPR-active species or a product derived from it induces DNA strand scission through an oxidative pathway in which the intermediacy of a hypervalent iron–oxo (ferryl, (Fe(IV)=O) or perferryl (Fe(V)=O)) unit has been implicated.[2b,2c] The Fe–BLM-induced DNA cleavage is sequence specific, and breaks are observed immediately following GC and GT (5′–3′) sequences. Both free bases and malondialdehyde-like materials are obtained as products of the DNA degradation.[4] Formation of these products has been shown to arise from a series of reactions initiated by C–H bond cleavage at the C4′ of the deoxyribose moieties of pyrimidine nucleotides adjacent to the guanosines.[2c] In addition to facile DNA cleavage, the Fe–BLM system also exhibits oxo-transfer activity.[2d,5] This latter property of Fe-BLM is rather unique since it is the first example of a non-heme system capable of O_2-activation. Recently, a series of non-heme, iron-containing enzymes has been identified that are involved in O_2-activation and exhibit mono- and/or dioxygenase activities.[6] Along with this pursuit, several reports on non-heme model iron complexes capable of O_2-activation have also appeared.[6–9] The model systems either consist of diiron centers ligated to designed ligands or involve diiron–oxo species as intermediates. Only in one case, spectroscopic evidences in favor of a mononuclear non-heme ferryl species resulting from peroxide-induced fragmentation of a diferric complex have been presented.[6]

(1) Blum, R. H.; Carter, S. K.; Agre, K. A. *Cancer* **1973**, *31*, 903.
(2) (a) Dedon, P. C.; Goldberg, I. H. *Chem. Res. Toxicol.* **1992**, *5*, 311. (b) Petering, D. H.; Byrnes, R. W.; Antholine, W. E. *Chem.-Biol. Interact.* **1990**, *73*, 133. (c) Stubbe, J.; Kozarich, J. W. *Chem. Rev.* **1987**, *87*, 1107. (d) Hecht, S. M. *Acc. Chem. Res.* **1986**, *19*, 383. (e) Sugiura, Y.; Takita, T.; Umezawa, H. *Met. Ions Biol. Syst.* **1985**, *19*, 81. (f) Dabrowiak, J. C. *Adv. Inorg. Biochem.* **1983**, *4*, 69.
(3) (a) Burger, R. M.; Kent, T. A.; Horwitz, S. B.; Munck, E.; Peisach, J. *J. Biol. Chem.* **1983**, *258*, 1559. (b) Burger, R. M.; Peisach, J.; Horwitz, S. B. *J. Biol. Chem.* **1981**, *256*, 11636.
(4) (a) Sausville, E. A.; Stein, R. W.; Peisach, J.; Horwitz, S. B. *Biochemistry* **1978**, *17*, 2746. (b) Sausville, E. A.; Peisach, J.; Horwitz, S. B. *Biochem. Biophys. Res. Commun.* **1976**, *73*, 814.
(5) (a) Heimbrook, D. C.; Carr, S. A.; Mentzer, M. A.; Long, E. C.; Hecht, S. M. *Inorg. Chem.* **1987**, *26*, 3835. (b) Heimbrook, D. C.; Mulholland, R. L.; Hecht, S. M. *J. Am. Chem. Soc.* **1986**, *108*, 7840. (c) Murugesan, N.; Hecht, S. M. *J. Am. Chem. Soc.* **1985**, *107*, 493. (d) Ehrenfeld, G. M.; Rodriguez, L. O.; Hecht, S. M.; Chang, C.; Basus, V. J.; Oppenheimer, N. J. *Biochemistry* **1985**, *24*, 81. (e) Ehrenfeld, G. M.; Murugesan, N.; Hecht, S. M. *Inorg. Chem.* **1984**, *23*, 1496.
(6) A good collection of references is included in the following: Leising, R. A.; Brennan, B. A.; Que, L., Jr.; Fox, B. G.; Munck, E. *J. Am. Chem. Soc.* **1991**, *113*, 3988.
(7) (a) Kitajima, N.; Ito, M.; Fukui, H.; Moro-oka, Y. *J. Chem. Soc., Chem. Commun.* **1991**, 102. (b) Stassinopoulos, A.; Caradonna, J. P. *J. Am. Chem. Soc.* **1990**, *112*, 7071.
(8) (a) Menage, S.; Brennan, B. A.; Juarez-Garcia, C.; Munck, E.; Que, L., Jr. *J. Am. Chem. Soc.* **1990**, *112*, 6423. (b) Leising, R. A.; Norman, R. E.; Que, L., Jr. *Inorg. Chem.* **1990**, *29*, 2553.
(9) (a) Sheu, C.; Sawyer, D. T. *J. Am. Chem. Soc.* **1990**, *112*, 8212. (b) Sheu, C.; Sobkowiak, A.; Jeon, S.; Sawyer, D. T. *J. Am. Chem. Soc.* **1990**, *112*, 879. (c) Cofre, P.; Richert, S. A.; Sobkowiak, A.; Sawyer, D. T. *Inorg. Chem.* **1990**, *29*, 2645.

0002-7863/93/1515-7971$04.00/0

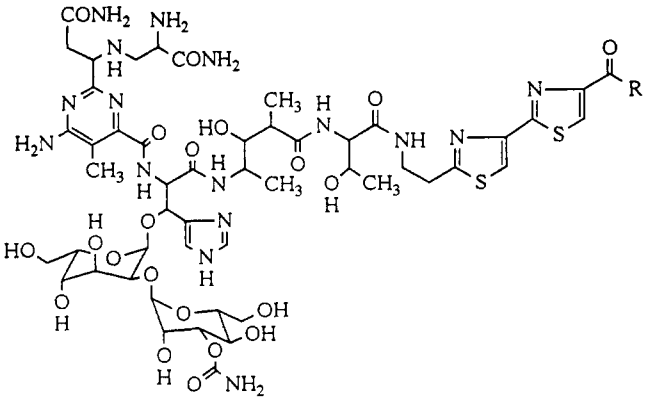

BLM (1)

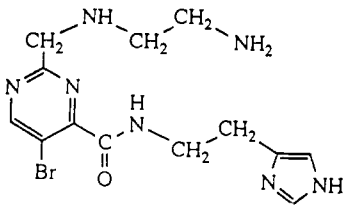

PMAH(2)

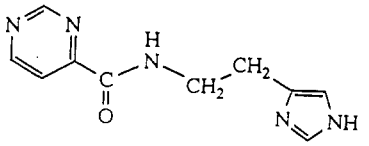

PrpepH (3)

In our attempts toward elucidation of the coordination structures and functions of metallobleomycins (M–BLMs), we have synthesized a designed ligand PMAH (**2**, H is the dissociable amide H) that mimics the metal-chelating domain of BLM. The structures of the Cu(II) complexes of this tailored ligand[10] and variations thereof[11] have established the structure of Cu(II)–BLM at physiological pH. Also, the Co(III) chelates of PMAH have indicated the differences in the set of donor atoms around cobalt in the so-called ORANGE, BROWN, and GREEN Co(III)–BLMs.[12] The results of the spectroscopic and kinetic studies as well as DNA cleavage reactions with these synthetic analogues have provided definitive suggestions regarding the mechanisms of the oxidative and photoinduced DNA damage by the corresponding M–BLMs.[12,13] In this article, we report the spectral properties and chemistry of the Fe(II) (**4**) and Fe(III) (**5**) complexes of PMAH. Under comparable reaction conditions, these two complexes give rise to EPR spectra identical to that of activated bleomycin. Also, like Fe–BLMs, **4** and **5** (a) promote rapid DNA strand scission with the production of base propenals and (b) exhibit very similar sequence specificity. The present complexes also comprise a set of *mononuclear* non-heme iron complexes that are capable of O_2-activation. As is the case with the Fe–BLMs, stereospecificity is observed in the oxo-transfer reactions by **4** and **5**. In addition to O-O bond scission in the oxo-transfer reactions, a rare example of O-O bond formation is noted in the reaction of **5** with iodosobenzene in presence of a base.

Experimental Section

Materials. PMAH and $[Fe(DMSO)_6](ClO_4)_3$·DMSO were synthesized according to the published procedures.[10,14] Blenoxane was a gift from the Cetus Corporation. The plasmid (ϕX174 (RF) and pBR322) DNAs, the restriction enzymes (*Nar*I and *Xma*III), and calf intestine alkaline phosphatase were purchased from the Bethesda Research Laboratories. T4 polynucleotide kinase was obtained from U.S. Biochemical Corporation. The Long-Ranger gel solution was procured from A-T Biochemicals. [γ-^{32}P]ATP was purchased from Amersham.

Preparation of Compounds. [Fe^{II}(PMA)]Cl·MeOH (4). Addition of 163 mg (1 mmol) of $FeCl_2·2H_2O$ to a mixture of 443 mg (1.2 mmol) of PMAH and 38 mg (1.2 mmol) of LiOMe in 30 mL of anhydrous methanol under dinitrogen resulted in a deep blue solution which was stirred for 8 h. Next, a solution of 1.65 g of Et_4NCl (10 mmol) in 10 mL of methanol was added, and the mixture was cooled at −20 °C for 20 h. [Fe^{II}(PMA)]-Cl·MeOH (**4**) was isolated as deep blue microcrystals in 25% yield. Anal. Calcd for $C_{14}H_{21}N_7O_2ClFe$: C, 34.28; H, 3.49; N, 19.99. Found: C, 34.26; H, 3.86; N, 19.69. Selected IR bands (KBr pellet, cm^{-1}): 3350-(s), 3147(s), 2910(m), 1590(vs, ν_{CO}), 1450(m), 1308(m), 1214(w), 1060-(m), 1020(m), 820(m).

[Fe^{III}(PMA)](NO$_3$)$_2$·DMSO (5). A slurry of 443 mg (1.2 mmol) of PMAH and 900 mg (1 mmol) of $[Fe(DMSO)_6](ClO_4)_3$·DMSO in 20 mL of acetonitrile was stirred under dinitrogen for 8 h. Slow addition of a solution of 580 mg (3 mmol) of $(Et_4N)(NO_3)$ in 10 mL of MeCN to the resulting deep red solution afforded red-brown microcrystals of [Fe^{III}(PMA)]$(NO_3)_2$·DMSO (**5**) in 90% yield. Anal. Calcd for $C_{15}H_{23}N_9O_8SFe$: C, 28.88; H, 3.70; N, 20.17. Found: C, 28.65; H, 3.87; N, 20.16. Selected IR bands (KBr pellet, cm^{-1}): 3425(s), 3130(s), 1666(m), 1630(s, ν_{CO}), 1560(w), 1350(vs, $\nu_{NO_3^-}$), 1098(s), 1028(m), 826-(m), 624(m). The more soluble perchlorate salt of [Fe^{III}(PMA)]$^{2+}$ was also isolated by the addition of $(Et_4N)(ClO_4)$ instead of $(Et_4N)(NO_3)$.

Electronic absorption spectrum (λ_{max}, nm, ϵ M^{-1} cm^{-1}) of **4** in methanol: 670 (2200), 620 sh (1950), 460 (900). Electron absorption spectrum of **5** in DMSO: 640 sh (300), 540 sh (900), 440 (1950).

Other Physical Measurements. Infrared spectra were obtained with a Perkin-Elmer 1600 FTIR spectrometer. Absorption spectra were measured on a Perkin-Elmer Lambda 9 spectrophotometer. A Bruker ESP-300 spectrometer was used to record the EPR spectra at X-band frequencies.

DNA Cleavage Experiments. DNA cleavage experiments were performed by mixing 1 μg of ϕX174 (RF) supercoiled covalently closed circular (ccc) DNA with 0.5 mM **4** and 10 mM sodium ascorbate. Equivalent samples also contained 0.3 mM DMSO (as radical scavanger). Reactions were carried out in pH 8 sodium cacodylate buffer, and the mixtures were exposed to air for 15, 30, and 60 min. Agarose gel (1%) electrophoreses were run (3 h) on a BRL H-5 horizontal gel system. Photographs were taken with a Polaroid MP-4 system following ethidium bromide staining. Densitometry on the negatives of the gel pictures was carried out with a Bio-Rad Model 620 video densitometer interfaced with a Compaq 386/20e computer.

Preparation of the 5′-End-Labeled Restriction Fragments.[15] pBR322 DNA was cleaved with the restriction endonuclease *Nar*I and dephosphorylated by the use of bacterial alkaline phosphatase. T4 polynucleotide kinase was then used to phosphorylate the free 5′-OH ends with [γ-^{32}P]-ATP. This step was followed by a final treatment with the restriction endonuclease *Xma*III. The labeled fragments were then separated by preparatory polyacrylamide gel electrophoresis. The fragments of choice (391- and 266-bp long) were excised and extracted by the "crush and soak" method.

(10) (a) Brown, S. J.; Hudson, S. E.; Stephan, D. W.; Mascharak, P. K. *Inorg. Chem.* **1989**, *28*, 468. (b) Brown, S. J.; Stephan, D. W.; Mascharak, P. K. *J. Am. Chem. Soc.* **1988**, *110*, 1996.

(11) Scheich, L. A.; Gosling, P.; Brown, S. J.; Olmstead, M. M.; Mascharak, P. K. *Inorg. Chem.* **1991**, *30*, 1677.

(12) (a) Tan, J. D.; Hudson, S. E.; Brown, S. J.; Olmstead, M. M.; Mascharak, P. K. *J. Am. Chem. Soc.* **1992**, *114*, 3841. (b) Brown, S. J.; Hudson, S. E.; Olmstead, M. M.; Mascharak, P. K. *J. Am. Chem. Soc.* **1989**, *111*, 6446.

(13) Hudson, S. E.; Mascharak, P. K. *Chem. Res. Toxicol.* **1989**, *2*, 411.

(14) Cotton, F. A.; Francis, R. *J. Am. Chem. Soc.* **1960**, *82*, 2986.

(15) Maniatis, T.; Fritsch, E. F.; Sambrook, J. *Molecular Cloning: A Laboratory Manual*; Cold Spring Harbor Laboratory Press: Cold Spring Harbor, NY, 1982.

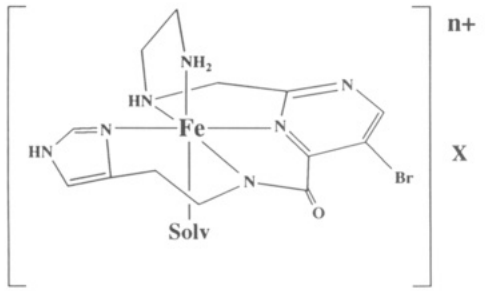

Complex 4, n = 1, X = Cl
Complex 5 n = 2, X = $(ClO_4)_2$ or $(NO_3)_2$

Figure 1. Structures of **4** and **5** as evidenced by the spectroscopic parameters.

Cleavage of the 5′-^{32}P-End-Labeled DNA Fragments. Reaction mixtures (25 μL total volume) contained 0.25 pmol (~2 × 10^4 cpm) of a 391- or 266-bp end-labeled DNA duplex and 1 μg of cold carrier pBR322 DNA in 10 mM sodium cacodylate buffer (pH 8) along with 50 μM Fe^{3+} (or Fe^{2+}), 50 μM PMAH (or BLM), and 300 μM H_2O_2. After initial preincubation (30 min) of the DNA mixtures with PMAH or BLM, H_2O_2 was added and reactions were initiated by the addition of incremental portions of iron. The samples were then allowed to react at room temperature for 30 min. Next, the reactions were quenched with Desferal (Ciba-Geigy), and the cleavage products were precipitated by the addition of yeast $tRNA^{Phe}$ (BRL) and ethanol. The precipitated DNA pellets were washed with ethanol, dried in vacuo, and redissolved in 98% formamide loading buffer. The samples were then heated at 90 °C for 10 min, quick-chilled, loaded on a 10% polyacrylamide denaturing (7 M urea) Long-Ranger gel, and electrophoresed at 1500 V for 2 h. The sequences were read with the help of standard Maxam-Gilbert sequencing fragments.

Thiobarbituric Assay.[16] Under dry N_2 atmosphere, the following reagents were combined: 0.2 mL of 20 mM sodium cacodylate buffer (pH 8), 0.2 mL of purified and sonicated calf thymus DNA (1 mg/mL) in water, 0.1 mL of **4** (2.5 mM) in sodium cacodylate buffer, and sodium ascorbate (to final concentration of 10 mM). Following 15-, 30-, and 60-min exposures to air, 0.5 mL of thiobarbituric acid (1% w/v in 0.05 M NaOH) and 0.5 mL of 28% trichloroacetic acid were added, and the contents were transferred to glass-stoppered flasks. These were then kept under hot water (90 °C) for 15 min. After the color was developed, the samples were extracted with 1.5 mL of 1-butanol, and their absorbances at 532 nm were recorded (ϵ_{532} = 1.6 × 10^5 M^{-1} cm^{-1}).

Oxo-Transfer Reactions. With stilbenes and naphthalene as substrates, detection of the oxo-transfer products was done by HPLC (Spectra Physics), while with cyclohexene, the products were detected by GC (Hewlett-Packard). Details of the experimental conditions either have been published[17] or are included in Table I.

Results and Discussion

The structures of **4** and **5** (Figure 1) have been assigned on the basis of their spectral parameters. We have previously reported the structures and properties of the Fe(II) and Fe(III) bis complexes of another designed ligand (PrpepH) (**3**), namely, [Fe(Prpep)$_2$] and [Fe(Prpep)$_2$]ClO_4, in which the three nitrogens located in the pyrimidine and imidazole rings as well as the *deprotonated peptido function* of the ligand are coordinated to the iron centers.[18] This mode of ligation is indicated by the ν_{CO} (1590 and 1630 cm^{-1}, respectively, for the Fe(II) and Fe(III) complexes of **3**) and strong charge-transfer bands in the visible region. Since **4** and **5** also exhibit ν_{CO} at 1590 and 1630 cm^{-1}, respectively, and display very similar charge-transfer bands, but with half the extinction coefficients (Figure 2), the pyrimidine–histamine–peptido moiety of PMAH has been shown to be ligated to the iron centers in these two complexes. Coordination by the amine groups of PMAH to iron is indicated by the N–H stretching frequencies and the EPR spectrum of **5**, which is typical of similar low-spin iron complexes.[19]

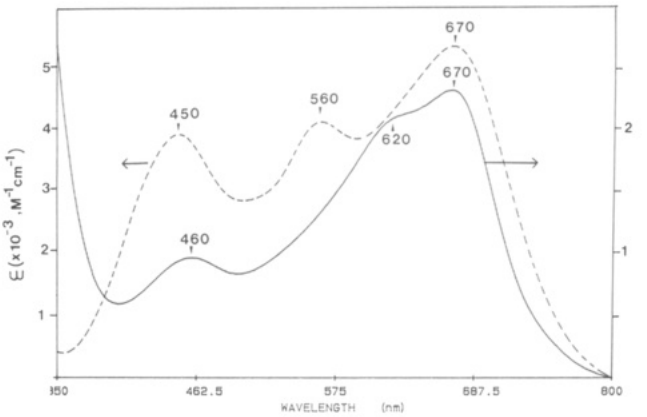

Figure 2. Electronic absorption spectra of **4** (solid line) and [Fe(Prpep)$_2$] (broken line) in methanol.

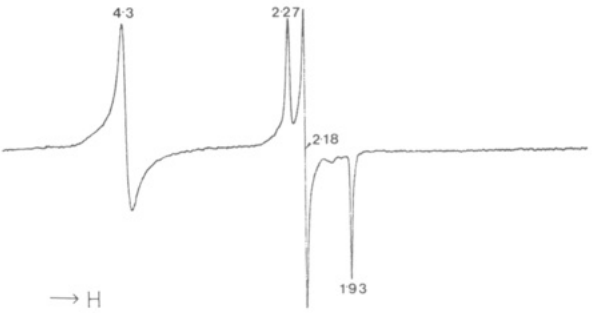

Figure 3. X-band EPR spectrum of **3** in methanol glass (100 K) following exposure (10 s) of the methanol solution to air before freezing. Selected *g* values are indicated. Spectrometer settings: microwave frequency, 9.43 GHz; microwave power, 12.9 mW; modulation frequency, 100 kHz; modulation amplitude, 2 G.

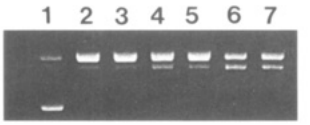

Figure 4. DNA (φX174 RF) cleavage by 0.5 mM [Fe^{II}(PMA)]$^+$ + 10 mM sodium ascorbate + O_2. Each reaction mixture contained 1 μg of DNA in a total volume of 25 μL of 20 mM cacodylate buffer (pH 8). Lane 1, DNA alone; lane 2, DNA + Fe complex + sodium ascorbate + O_2 exposure (15 min); lane 3, same as lane 2 except for added DMSO (0.3 mM); lane 4, same as lane 2 except for 30-min exposure to O_2; lane 5, same as lane 3 except for 30-min exposure to O_2; lane 6, same as lane 2 except for 60-min exposure to O_2; lane 7, same as lane 3 except for 60-min exposure to O_2.

Ligation of the deprotonated PMA^- framework to iron in the pentadentate manner (as shown in Figure 1) is also indicated by the reactions of CO and NO with **4**. In both cases, the entering ligand binds at the sixth site on iron. Passage of CO through a methanolic solution of **4** brings about a rapid color change from deep blue to green. Addition of excess $LiClO_4$ to such solution affords the CO adduct as a dark green solid which exhibits ν_{CO} at 1970 cm^{-1}, much within the range observed with mono CO adducts of Fe(II) complexes of tetraethylenepentamine and porphyrins.[20] Purging of the deep green solution of the CO adduct

(16) (a) Quinlan, G. J.; Gutteridge, J. M. C. *Biochem. Pharmacol.* **1987**, *36*, 3629. (b) Giloni, L.; Takeshita, M.; Johnson, F.; Iden, C.; Grollman, A. P. *J. Biol. Chem.* **1981**, *256*, 8608.
(17) Dawson, D. Y.; Hudson, S. E.; Mascharak, P. K. *J. Inorg. Biochem.* **1992**, *47*, 109.
(18) Brown, S. J.; Olmstead, M. M.; Mascharak, P. K. *Inorg. Chem.* **1990**, *29*, 3229.
(19) Sugiura, Y. *J. Am. Chem. Soc.* **1980**, *102*, 5208.
(20) (a) Melby, L. R. *Inorg. Chem.* **1970**, *9*, 2186. (b) Wayland, B. B.; Mehne, L. F.; Swartz, J. *J. Am. Chem. Soc.* **1978**, *100*, 2379. (c) Vaska, L.; Yamaji, T. *J. Am. Chem. Soc.* **1971**, *93*, 6673.
(21) (a) Akkerman, M. A. J.; Neijman, E. W. J. F.; Wijmenga, S. S.; Hilbers, C. W.; Bermel, W. *J. Am. Chem. Soc.* **1990**, *112*, 7462. (b) Oppenheimer, N. J.; Rodriguez, L. O.; Hecht, S. M. *Proc. Natl. Acad. Sci. U.S.A.* **1979**, *76*, 5616.

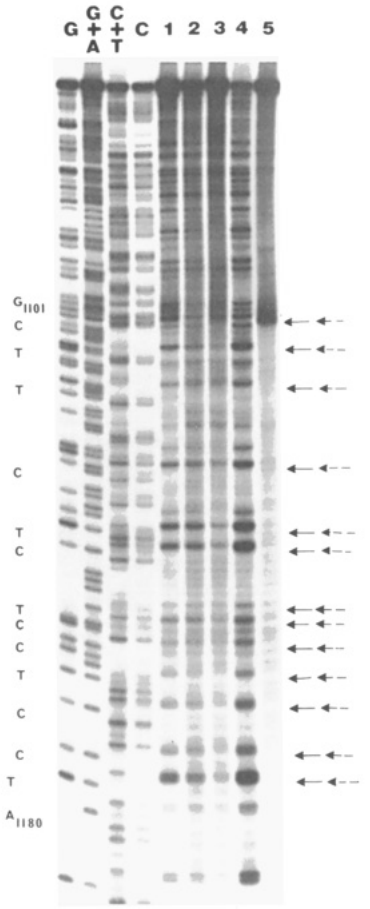

Figure 5. Autoradiogram of a 10% polyacrylamide/7 M urea gel showing the sequence specificities observed in DNA cleavage reactions by **5** and Fe(III)–BLM in presence of H_2O_2. A 266-bp 5-^{32}P-end-labeled fragment of pBR322 DNA was used. Lanes G, G + A, C + T, and C show the products of the respective Maxam-Gilbert sequencing reactions. Lane 1, 4 μM Fe(II)–BLM + O_2; lanes 2 and 3, 50 and 25 μM **5** with 300 μM H_2O_2, respectively; lane 4, 10 μM Fe(III)–BLM with 300 μM H_2O_2; lane 5, 50 μM Fe^{2+} + 300 μM H_2O_2. Only lane 1 contained 10 mM sodium ascorbate. The arrows indicate selected BLM and PMAH cleavage sites.

with dry N_2 regenerates the original blue solution of **4**. This confirms the fact that **4**, like Fe(II)–BLM,[21] binds CO reversibly. Also, the ν_{CO} frequency of Fe(II)–PMA–CO is very close to the value determined for the Fe(II)–BLM–CO adduct in D_2O (1973 cm^{-1}).[22] The NO adduct of **4** is readily obtained by bubbling NO through a solution of **4** in methanol. The EPR spectrum of the NO adduct is rhombic, with a triplet ^{14}N hyperfine splitting in the central g_z signal, and is typical of the six-coordinate type.[23] The EPR parameters (g_x = 2.04, g_y = 1.97, g_z = 2.007, A^N = 25 G) are also very similar to those of Fe(II)–BLM–NO (g_x = 2.041, g_y = 1.976, g_z = 2.008, A^N = 23.6 G).[19,24]

Brief exposure ($\lesssim$30 s) of the deep blue methanolic solution of **4** to air generates an oxygenated species that exhibits strong EPR signals with g = 2.27, 2.18, and 1.93 (Figure 3, signal A hereafter). The same spectrum is obtained with activated bleomycin.[3b] Signal A arises from a peroxo-bound low-spin rhombic Fe(III) center [(PMA)Fe(III)–O–OH]$^+$ in the oxygenated solution.[19,20,25] The second electron needed for the formation of the peroxo unit on iron in [(PMA)Fe(III)–O–OH]$^+$ is provided by a second $[Fe^{II}(PMA)]^+$ ion, which in turn is converted into a high-spin Fe(III) species (g = 4.3, Figure 3). Spin integration measurements confirm the 1:1 ratio of the g = 4.3 signal and signal A.[26] Signal A is also observed when **5** is allowed to react with H_2O_2 in DMSO. It is important to note that **4** gives rise to signal A under conditions that are very similar to those for the formation of activated bleomycin.[3] The only difference is the in situ formation of a low-spin (BLM)–Fe(III)–OH complex (in 1:1 ratio) during production of activated bleomycin via oxygenation of Fe(II)–BLM[3b,19]; in the case of **4**, a high-spin Fe(III) species is obtained instead. Interestingly, oxygenation of the Fe(II) complex of deglyco-BLM also affords activated bleomycin (in low yield) with no low-spin Fe(III) species.[27]

Attempts to confirm the presence of the coordinated hydroperoxide in [(PMA)Fe(III)–O–OH]$^+$ (species responsible for signal A) by resonance Raman spectroscopy have so far been unsuccessful. Resonance Raman experiments with [(PMA)Fe(III)–O–OH]$^+$ in methanol glass (liquid N_2 temperature) afforded inconclusive results due to (a) no resonance enhancement and hence very weak signals and (b) extensive photoreduction. Photoreduction of Fe(III)–BLM has been reported by two groups.[28] We have, therefore, sought chemical evidence in favor of the coordinated hydroperoxide in [(PMA)Fe(III)–O–OH]$^+$. In three separate tests with ferricyanide,[29] ferrothiocyanate, and KI,[30] [(PMA)Fe(III)–O–OH]$^+$ provided positive responses.[31] These results, along with the EPR spectra, strongly suggest that activated bleomycin is indeed the peroxy adduct of Fe(III)–BLM. A recent review on BLM also supports this assignment.[2b]

Solution of [(PMA)Fe(III)–O–OH]$^+$ in methanol is stable for several h at liquid N_2 temperature. At 0 °C, both g = 4.3 and signal A disappear within 3 h and a brown precipitate is observed. Cleavage of the O–O bond in [(PMA)Fe(III)–O–OH]$^+$ is expected to generate a hypervalent iron–oxo species in solution.[2,32] That a strongly oxidizing species is indeed present in such solution is evidenced by (a) formation of $^{\bullet}CH_2OH$ radical (detected by spin trapping, A^H = 22.7 G, A^N = 16 G[33]), (b) production of formaldehyde (detected by Nash reagent[34]), and (c) appearance of ESR signal from a diffusible peroxy radical (g = 2.22 and 2.05), most probably $^{\bullet}OOCH_2OH$, within minutes (Figure S1, supplementary material). Reaction of O_2 with $^{\bullet}CH_2OH$ (derived from CH_3OH via H atom abstraction by the highly oxidizing unit) could produce this peroxy species in solution.

Similarities in spectroscopic properties between individual iron complexes of BLM and the corresponding model complexes of PMAH (**4** and **5**) prompted us to study the DNA strand scission reactions with **4** and **5**. Incubation of supercoiled ccc (from I) ϕX174 DNA with submillimolar **4** in presence of O_2 (and ascorbate as the reducing agent for multiple turnover) results in rapid appearance (within 10 min) of nicked circular (form II) and linear duplex (form III) DNA (Figure 4; lanes 2, 4, and 6).

(22) Sugiura, Y.; Kuwahara, J.; Suzuki, T. *FEBS Lett.* **1985**, *182*, 39.
(23) Kon, H. *Biochim. Biophys. Acta* **1975**, *379*, 103.
(24) Sugiura, Y.; Ishizu, K. *J. Inorg. Biochem.* **1979**, *11*, 171.
(25) For EPR parameters of low-spin non-heme Fe(III) complexes, see: (a) Stynes, D. V.; Noglik, H.; Thompson, D. W. *Inorg. Chem.* **1991**, *30*, 4567. (b) McDevitt, M. R.; Addison, A. W.; Sinn, E.; Thompson, L. K. *Inorg. Chem.* **1990**, *29*, 3425. (c) Tajima, K. *Inorg. Chim. Acta* **1990**, *169*, 211; **1989**, *163*, 115. (d) Sugiura, Y.; Kuwahara, J.; Nagasawa, T.; Yamada, H. *J. Am. Chem. Soc.* **1987**, *109*, 5848.
(26) Na[Fe(EDTA)]·4H_2O (S = $^5/_2$) and [Cu(PMA)](BF_4) (S = $^1/_2$) were used as standards in the spin integration measurements. Authetic samples were dissolved in aqueous glycerol (7:3), and the EPR signals at 100 K were integrated by using the software package on the Bruker ESP-300 machine.
(27) Kenani, A.; Bailly, C.; Helbecque, N.; Catteau, J. P.; Houssin, R.; Bernier, J. L.; Henichart, J. P. *Biochem. J.* **1988**, *253*, 497.
(28) (a) Burger, R. M.; Peisach, J. *Inorg. Chim. Acta* **1983**, *79*, 304. (b) Sugiura, Y.; Suzuki, T.; Kuwahara, J.; Tanaka, H. *Biochem. Biophys. Res. Commun.* **1982**, *105*, 1511.
(29) Chang, C. H.; Dallas, J. L.; Meares, C. F. *Biochem. Biophys. Res. Commun.* **1983**, *110*, 959.
(30) Gordon, A. J.; Ford, R. A. *The Chemist's Companion*; Wiley: New York, NY, 1972.
(31) [(PMA)Fe(III)–O–OH]$^+$ is quite reactive and decomposes rapidly at room temperature. Expectedly, titrations of the methanolic solutions of [(PMA)Fe(III)–O–OH]$^+$ with aqueous KI as well as the spectrophotometric determinations with ferricyanide indicated 0.5–0.8 equiv of peroxide in [(PMA)Fe(III)–O–OH]$^+$ in four separate measurements.
(32) McMurry, T. J.; Groves, J. T. In *Cytochrome P-450: Structure, Mechanism, and Biochemistry*; Ortiz de Montellano, P. R., Ed.; Plenum: New York, 1986; p 3 and references therein.
(33) Marriot, P. R.; Perkins, M. J.; Griller, D. *Can. J. Chem.* **1980**, *58*, 803.
(34) Nash, T. *Biochem. J.* **1953**, *55*, 416.

Table I. Results of Oxo-Transfer Reactions in $CH_3CN/H_2O/CH_3OH$ Media[a]

oxidant	complex	products[d] *cis*-stilbene oxide	*trans*-stilbene oxide	benz-aldehyde	deoxy-benzoin
		cis-Stilbene			
PhIO[b]	[Fe(TPP)]Cl	26	2.5	0.1	0.3
	[Fe(III)(PMA)](ClO$_4$)$_2$ (**5**)	15.8	2.3	0.2	2.0
	[Fe(III)(BLM)](ClO$_4$)$_2$[f]	20.0	8.0	5.0	5.0
H_2O_2[c]	[Fe(TPP)]Cl	265	6.6	11.3	0.8
	[Fe(III)(PMA)](ClO$_4$)$_2$ (**5**)	73	7.3	27	4.3
O_2[c]	[Fe(II)(PMA)]Cl (**4**)	10	1.2	7	0.5
		trans-Stilbene			
PhIO[b]	[Fe(TPP)]Cl		11.3	0.1	0.02
	[Fe(III)(PMA)](ClO$_4$)$_2$ (**5**)		10.6	0.5	0.03
	[Fe(III)(BLM)](ClO$_4$)$_2$[f]		3.0	0.0	2.0
H_2O_2[c]	[Fe(TPP)]Cl		34.0	5.9	11.4
	[Fe(III)(PMA)](ClO$_4$)$_2$ (**5**)		40.0	14.6	2.4
O_2[c]	[Fe(II)(PMA)]Cl (**4**)		5.3	1.2	0.4

oxidant	complex	Products[e] cyclohexene oxide	2-cyclo-hexen-1-one	2-cyclo-hexen-1-ol
		Cyclohexene		
PhIO[b]	[Fe(TPP)]Cl	61	7.1	5.2
	[Fe(III)(PMA)](ClO$_4$)$_2$ (**5**)	37	3.5	4.9
	[Fe(III)(BLM)](ClO$_4$)$_2$[f]	9	trace	12
H_2O_2[c]	[Fe(TPP)]Cl	2.3×10^3	314	33
	[Fe(III)(PMA)](ClO$_4$)$_2$ (**5**)	2.8×10^2	57.3	8.3
O_2[c]	[Fe(II)(PMA)]Cl (**4**)	165	159	10.9

oxidant	complex	product[d] α-naphthol
	Naphthalene	
PhIO[b]	[Fe(TPP)]Cl	70
	[Fe(III)(PMA)](ClO$_4$)$_2$ (**5**)	216
H_2O_2[c]	[Fe(TPP)]Cl	246
	[Fe(III)(PMA)](ClO$_4$)$_2$ (**5**)	62
O_2[c]	[Fe(II)(PMA)]Cl (**4**)	200
	[Fe(II)(BLM)][f]	162

[a] Capacities of oxo transfer by Fe(II) and Fe(III) perchlorates under the reaction conditions were extremely low. [b] Yields based on PhIO. [c] Yields based on metal complex. [d] HPLC, $CH_3CN:H_2O$, 70:30; 250-mm C18 Econosphere column, UV detection. [e] GC, DB5 column, FID detection. [f] Reference 5c. Reaction mixtures of **4** and substrates also contained 10 mM sodium ascorbate.

Longer incubation leads to digestion of DNA with the formation of base propenals[4] (indicated by thiobarbituric acid assay[16]). The progressive appearance of the linear duplex (form III) in Figure 4 suggests significant association of the model complex with DNA, enough for at least two oxidative events in close proximity. The extent of DNA strand scission is reduced only slightly in the presence of DMSO (Figure 4; lanes 3, 5, and 7), a fact that rules out the possibility of catalytic production of •OH radical in the incubation medium.[35] DNA cleavage is also observed with **5** and H_2O_2. Since base propenals are obtained in DNA strand scission reactions by both **4** and **5**, the mechanism of the oxidative damage of DNA by these model complexes is likely to be quite similar to that proposed for Fe–BLMs.[2c]

Recently, it has been argued that although the bithiazole terminus of BLM is responsible for strong DNA binding, the primary determinant of the DNA sequence specificity of Fe–BLM is the metal-binding domain.[36] The present complexes **4** and **5**, being devoid of any DNA-binding moiety, are ideal

Scheme I. Sequence-Specific Cleavage Sites Observed in the DNA Strand Scission Reactions[a]

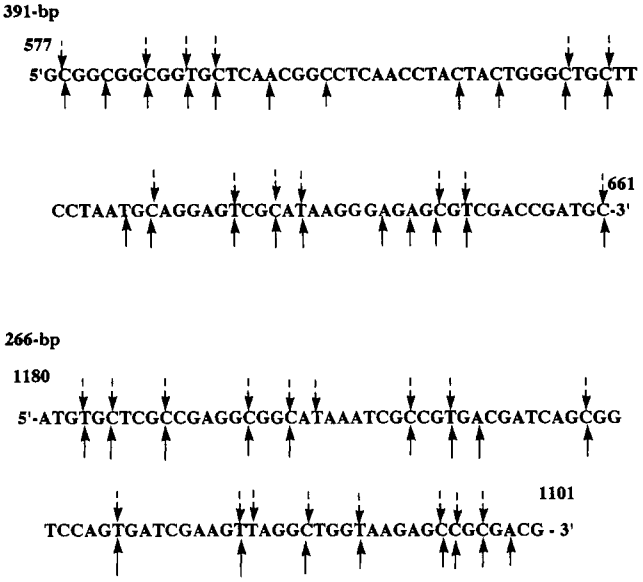

[a] The solid and broken arrows indicate BLM and PMAH sites, respectively.

candidates for testing this hypothesis. The DNA cleavage activity of **4** and **5** confirms electrostatic binding of the cationic complexes **4** and **5** to DNA. We have, therefore, studied the sequence specificity of **4** and **5** and compared it (if any) with that of the Fe–BLMs. Surprisingly, the sequence specificity observed in the DNA cleavage reactions by the model complexes is almost identical to that exhibited by the Fe-BLMs. Degradation of the 266-bp restriction fragment by 50 μM **5** + 300 μM H_2O_2 is illustrated in Figure 5. In the 79-bp region from 5'-A_{1180} to 3'-G_{1101}, Fe(III)–BLM exhibits 17 major cleavage sites, 15 of which are also observed with **5**. It is interesting to note that all GC and GT (5'–3') cleavage sites of Fe–BLM are cleaved by **5**, while the GA (5'–3') sites are preferred by Fe–BLM only (Scheme I). With the 391-bp fragment, similar results are obtained (not shown in Figure 5). The 90-bp region from 5'-A_{570} to 3'-C_{661} displays 21 cleavage sites with Fe–BLM, 13 of which are identical to those exhibited by **5**. Here, also, the GC and GT (5'–3') sites (but not GA (5'–3')) are duplicated (Scheme I). Taken together, these DNA cleavage reactions suggest that (a) **4** and **5** are indeed very good models of the metalated domain of Fe–BLM and (b)the metal-chelating domain of BLM plays a dominant role in the sequence-dependent binding of the drug.

Hecht and co-workers have reported catalytic oxygen transfer to olefinic substrates by the iron complexes of BLM.[5] The extent of oxo transfer is significant with Fe(III)–BLM and an oxygen surrogate like iodosobenzene, while with Fe(II)–BLM + O_2 + ascorbate, low yields of the oxygenated products are obtained. This group has compared the oxo-transfer reactions of Fe–BLMs with reactions of cytochrome P-450 and has proposed a similar mechanism that involves perferryl intermediates. Shown in Table I are the results of the oxo-transfer reactions of **4** and **5** along with [Fe(TPP)]Cl (TPP = tetraphenylporphyrinato). It is clear that **4** and **5** are effective oxo-transfer agents and the efficiencies of oxo transfer to a variety of substrates approach that of the heme analogue [Fe(TPP)]Cl under virtually identical conditions. Simple iron salts and iron complexes of simpler analogues like PrpepH (**3**) are ineffective as oxo-transfer agents under the conditions mentioned in Table I. In a previous report,[17] results of the oxo-transfer reactions of **4** and **5** with various oxidants and stilbenes as substrates have been discussed. The present study is more complete, and the reaction conditions are optimized especially in cases where dioxygen has been used as the oxidant.

Formation of the oxo-transfer products of Table I indicates

(35) Shepherd, R. E.; Lomis, T. J.; Koepsel, R. R. *J. Chem. Soc., Chem. Commun.* **1992**, *222*.

(36) (a) Carter, B. J.; Murty, V. S.; Reddy, K. S.; Wang, S. N.; Hecht, S. M. *J. Biol. Chem.* **1990**, *265*, 4193. (b) Shipley, J. B.; Hecht, S. M. *Chem. Res. Toxicol.* **1988**, *1*, 25. (c) Sugiyama, H.; Kilkuskie, R. E.; Chang, L. H.; Ma, L. T.; Hecht, S. M.; van der Marel, G. A.; van Boom, J. H. *J. Am. Chem. Soc.* **1986**, *108*, 3852.

eventual heterolytic cleavage of the O–O bond in [(PMA)Fe(III)–O–OH]$^+$ to produce the perferryl (Fe(V)=O) intermediate in the reaction mixtures. With *cis*-stilbene, concerted transfer of the oxo unit by the perferryl intermediate generates the *cis*-oxide (stereospecificity retained), while rotation around the C–C bond in the transition state of the stepwise electrophilic pathway[5c] leads to the formation of a small amount of the *trans*-oxide. It is important to note that *trans*-stilbene affords only the *trans*-oxide. Such stereospecificy is exhibited by the Fe–BLMs, [Fe(TPP)]$^+$, and among model complexes only by **4** and **5**. The presence of the perferryl intermediate is further supported by the fact that both **4** and **5** convert *N*,*N*-dimethylaniline to *N*-methylaniline with a corresponding positive test for formaldehyde.[5c] Formation of high amounts of benzaldehyde under aerobic conditions indicates the presence of the stilbene cation radical[5b] in the reaction mixtures. Abstraction of one electron by the perferryl intermediate gives rise to this cation radical, which in turn reacts with dioxygen to form benzaldehyde via a dioxetane intermediate. Additional discussions on these reaction pathways can be found in refs 5 and 17.

When cyclohexene is used as the substrate, two minor products, namely, 2-cyclohexen-1-one and 2-cyclohexen-1-ol, are also obtained along with cyclohexene oxide. Free-radical chemistry can account for the formation of these minor products. The allylic C–H bond in cyclohexene is weaker (bond energy = 87 kcal/mol) compared to both the vinylic C–H (bond energy = 108 kcal/mol) and the alkyl C–H (bond energy = 95 kcal/mol) bonds.[37] This fact allows preferential generation of the allylic radical as a result of H atom abstraction by the perferryl intermediate. Combination of the allylic radical with $^{\bullet}$OH affords 2-cyclohexen-1-ol, while reaction of the same with O_2 produces 2-cyclohexen-1-one via a peroxy intermediate. Oxo-transfer reactions with naphthalene afford α-naphthol as the sole product.[38] This product most probably results from initial H atom abstraction by the perferryl intermediate. Greater stability of the naphthyl radical with the single electron at the α-position could account for the singular product. Studies on the mechanisms of all these oxo-transfer reactions, including ^{18}O-labeling experiments, are in progress in this laboratory, and the results will be reported in due time elsewhere.

Comparisons of the product distributions of the various oxo-transfer reactions of **4** and **5** with those of Fe–BLMs (Table I) clearly indicate that the model complexes possess comparable oxo-transfer capabilities. Unlike some earlier synthetic analogues of BLM,[39] iron complexes of PMAH exhibit more pronounced stereospecificity in the oxo-transfer reactions with the stilbenes. The iron complexes of a set of pyridine-based analogues of BLM that exhibit moderate oxo-transfer capabilities have been reported recently.[40] However, unlike **4** and **5**, these model complexes generate very high concentrations of $^{\bullet}$OH radical, and several active species have been proposed as intermediates in their oxo-transfer reactions.

To date, all model complexes of Fe–BLMs have been generated in situ. In contrast, the present complexes **4** and **5** have been isolated as analytically pure solids and are much better characterized. They also mimic BLM chemistry more closely and exhibit clean oxo-transfer reactions. The latter property of these complexes is especially noteworthy, since **4** and **5** are the first

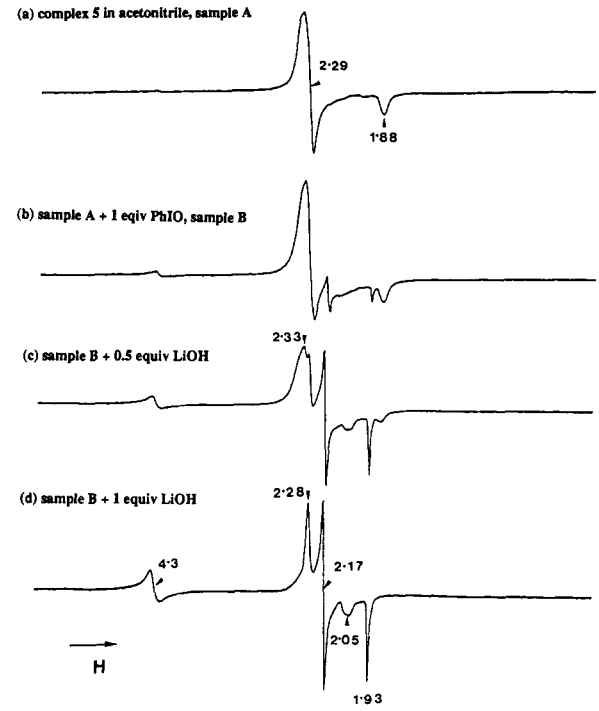

Figure 6. X-band EPR spectra (100 K) of **5** (trace a), **5** + 1 equiv of PhIO (trace b), **5** + 1 equiv of PhIO + 0.5 equiv of LiOH (trace c), and **5** + 1 equiv of PhIO + 1 equiv of LiOH (trace d) in acetonitrile/methanol glass. For spectrometer settings, see Figure 3.

examples of *mononuclear* non-heme iron complexes that exhibit monooxygenase activity. There is no sign of any dimeric active catalyst in the oxo-transfer reactions of these complexes.

It must be mentioned here that though formation of the products of Table I has been rationalized on the basis of a perferryl intermediate, we (and others[2-5]) have failed to obtain any direct evidence to confirm the presence of such an intermediate in any case. It is quite possible that the {hydroperoxo}Fe(III) intermediate observed with **4** and **5** under the experimental conditions is the source of the catalytic activity. This {hydroperoxo}Fe(III) species could lead to multiple reaction pathways including production of the perferryl unit. For example, the {hydroperoxo}-Fe(III) (and not the perferryl) intermediate could abstract H atom from the olefinic substrates and lead to several products of Table I. The presence of large concentrations of $^{\bullet}$CH$_2$OH radical and formaldehyde in the methanolic solution of [(PMA)Fe(III)–O–OH]$^+$ supports this hypothesis. It is quite possible that such {hydroperoxo}Fe(III) species is involved in oxygen-activation by non-heme iron complexes in general. In a recent article, Busch and co-workers have raised this issue and provided some experimental evidences in its favor.[41]

Finally, we report a rare example of O–O bond formation (reverse of the monooxygenase activity) in the reaction between **5** and PhIO in basic medium. A strictly anaerobic solution of **5** in acetonitrile exhibits an axial EPR spectrum with $g_\perp = 2.29$ and $g_\parallel = 1.88$ (Figure 6a). Addition of 1 equiv of PhIO (dissolved in methanol) to this solution causes minor changes and the appearance of weak signals around $g = 2$ (Figure 6b). Further addition of LiOH to this mixture rapidly generates signal A (Figure 6c) with the maximum intensity at the point at which exactly 1 equiv of LiOH has been added (Figure 6d). Formation of signal A in this experiment can be rationalized in terms of the unusual reaction 1, which indicates O–O bond formation at the iron center of **5**. In the presence of a small amount of water in the reaction mixture, other bases like LiOMe or even PMAH bring about the same chemical change. We are aware of one

(37) McMurry, J. *Organic Chemistry*, 2nd ed.; Brooks Cole: Pacific Grove, CA, 1988; p 311.

(38) Fe(III)–BLM + PhIO produces mixtures of polyoxygenated phenols in aqueous methanol.[5c]

(39) Kilkuskie, R. E.; Suguna, H.; Yellin, B.; Murugesan, N.; Hecht, S. M. *J. Am. Chem. Soc.* **1985**, *107*, 260.

(40) (a) Suga, A.; Sugiyama, T.; Otsuka, M.; Ohno, M.; Sugiura, Y.; Maeda, K. *Tetrahedron* **1991**, *47*, 1191. (b) Ohno, M.; Otsuka, M. In *Stereochemistry of Organic and Bioorganic Transformations: Proceedings of the Seventeenth Workshop Conference Hoechst, Schloss Reisensburg*; Bartmann, W., Sharpless, K. B., Eds.; VCH: New York, 1987. (c) Sugano, Y.; Kittaka, A.; Otsuka, M.; Ohno, M.; Sugiura, Y.; Umezawa, H. *Tetrahedron Lett.* **1986**, *27*, 3635.

(41) Sauer-Masarwa, A.; Herron, N.; Fendrick, C. M.; Busch, D. H. *Inorg. Chem.* **1993**, *32*, 1086.

$$[Fe^{III}(PMA)]^{2+} + PhIO + OH^- \rightarrow [(PMA)Fe(III)\text{–}O\text{–}OH]^+ + PhI \quad (1)$$

other example of such a transformation. Busch and co-workers have reported O–O bond formation in reactions of Fe(III) cyclidines with PhIO in basic solutions containing a small amount of water.[41] Apart from being an important reaction to be studied for its own merit, reaction 1 also suggests that [(PMA)Fe(III)–O–OH]$^+$ could be the active catalyst in the oxo-transfer reactions by the **5** + PhIO system.

Acknowledgment. Financial assistance from the American Cancer Society (CH-481) and the National Cancer Institute (CA 53076) is gratefully acknowledged. R.J.G. was supported by a NIH-MBRS grant (GM08132).

Supplementary Material Available: ESR spectrum of $^{\bullet}OOCH_2OH$ radical produced along with signal A in methanol (Figure S1) (1 page). Ordering information is given on any current masthead page.